AAC Accepts, published online ahead of print on 3 November 2014
Antimicrob. Agents Chemother. doi:10.1128/AAC.03342-14

A chemical rescue screen identifies a *Plasmodium falciparum* apicoplast inhibitor targeting MEP isoprenoid precursor biosynthesis

Wesley Wu[4], Zachary Herrera[1], Danny Ebert[4], Katie Baska[1], Seok H. Cho[4], Joseph L. DeRisi[4,5,*], Ellen Yeh[1,2,3,*]

[1]Department of Biochemistry, [2]Pathology, and [3]Microbiology and Immunology, Stanford Medical School, Stanford, CA, USA

[4]Department of Biochemistry and Biophysics, University of California, San Francisco, CA, USA

[5]Howard Hughes Medical Institute, Chevy Chase, MD, USA

Running head: Plasmodium apicoplast MEP pathway inhibitor

*Address correspondence to Ellen Yeh, ellenyeh@stanford.edu and Joseph DeRisi, joe@derisilab.ucsf.edu

Abstract

The apicoplast is an essential plastid organelle found in *Plasmodium* spp parasites, which contains several clinically validated anti-malarial drug targets. A chemical rescue screen identified MMV-08138 from the "Malaria Box" library of growth-inhibitory anti-malarial compounds as having specific activity against the apicoplast. MMV-08138 inhibition of blood-stage *P. falciparum* growth is stereospecific and potent, with the most active diastereomer demonstrating an EC_{50}=110 nM. Whole-genome sequencing of 3 drug-resistant parasite populations from two independent selections revealed E688Q and L244I mutations in *P. falciparum* IspD, an enzyme in the MEP isoprenoid precursor biosynthesis pathway in the apicoplast. The active diastereomer of MMV-08138 directly inhibited PfIspD activity *in vitro* with an IC_{50} of 7.0 nM. MMV-08138 is the first PfIspD inhibitor to be identified and, together with heterologously expressed PfIspD, provides the foundation for further development of this promising anti-malarial drug candidate lead. Furthermore, this study validates the use of the apicoplast chemical rescue screen coupled with target elucidation as a discovery tool to identify specific apicoplast-targeting compounds with new mechanisms of action.

Introduction

Despite encouraging progress over the past decade, malaria caused by *Plasmodium* spp parasites continues to pose an enormous disease burden (1). New anti-malarials with novel mechanisms of action are needed to circumvent existing or emerging drug resistance (2). The apicoplast is a plastid organelle unique to *Plasmodium* spp (and other pathogenic Apicomplexa parasites) and a key target for development of new anti-malarials. Due to its prokaryotic origin and evolution as a secondary plastid, it contains pathways that have no counterpart in the human host (3, 4). In *Plasmodium*, the apicoplast is essential for both intraerythrocytic and intrahepatic development in the human host (5, 6).

Despite efforts to develop inhibitors of apicoplast function, to date, there are no primary agents for treatment of acute malaria whose mechanism of action targets this unusual plastid organelle. Antibiotics that inhibit prokaryotic transcription and translation, such as doxycycline and clindamycin, block expression of the apicoplast genome and are active against *Plasmodium* parasites (5). Unfortunately, these drugs show a "delayed death" phenotype, in which growth inhibition occurs only after 2 replication cycles (96 hours). The slow kinetics limit the use of doxycycline and clindamycin to chemoprophylaxis or as a partner drug in combination therapies with faster-acting compounds. Fosmidomycin, which inhibits the enzyme DoxR/IspC for MEP isoprenoid precursor biosynthesis in the apicoplast, has immediate onset but shows high recrudescence rates clinically when used as monotherapy (7, 8). The efficacy of fosmidomycin-based combination therapy is currently being evaluated with mixed results (9–12). Development of new apicoplast inhibitors as anti-malarials has been challenging due to gaps in our knowledge of apicoplast biology and specific pathways and proteins to target.

As an alternative to target-specific approaches, several large-scale "chemical genetics" screens have been carried out to identify compounds with anti-malarial activity, defined by growth inhibition of *P. falciparum* blood cultures (13–15). This approach 1) directly measures a disease-relevant phenotype while 2) interrogating all cellular pathways in 3) an unbiased manner to identify the most drug-sensitive nodes, even if the target proteins were not previously obvious or even characterized (16). Forward chemical genetics is particularly useful in *Plasmodium*, where the lack of practical methods for large-scale mutant analysis to deconvolute new pathways or conditional knockouts to investigate essential functions prohibits genetic approaches that have been so powerful in the past in other model systems (17). However, major drawbacks to this approach are that, once a compound is identified as growth inhibitory, its target protein or pathway may be difficult to decipher and may be one of multiple targets if the compound is non-specific (16).

Our previous work demonstrated that the essential function of the apicoplast in *P. falciparum* blood-stage parasites is the production of isoprenoid precursors, isopentenyl pyrophosphate (IPP) and its isomer dimethylallyl pyrophosphate (DMAPP), by the prokaryotic MEP pathway (18). The remaining plastid pathways are required to house this critical biosynthetic activity and to supply it with cofactors and substrates. We demonstrated this by generating *P. falciparum* parasites that lacked apicoplasts but could be chemically rescued by addition of IPP to the growth media. The IPP chemical rescue presents an exciting opportunity to carry out a simple pathway-specific screen to identify small molecules that target the apicoplast. Compounds whose anti-malarial growth inhibition is eliminated by the addition of IPP would be revealed to target essential pathways for apicoplast function. IPP has already been shown to rescue growth inhibition by fosmidomycin and antibiotics (18). This chemical rescue screen

retains all the benefits of an unbiased, phenotypic screen but overcomes the main drawbacks by 1) ensuring specificity and 2) providing important insight into the biological target and mechanism of action.

In principle, a chemical rescue screen, followed by target elucidation, enables discovery of apicoplast inhibitors with new mechanisms of action. However, this strategy has yet to be proven as a discovery tool. Recently, the inhibitor MMV-08138 was identified by an IPP chemical rescue screen as having specific activity against the apicoplast (19, 20). Unfortunately, the target of the inhibitor was unknown and therefore the mechanism of apicoplast dysfunction was unclear. Herein, we provide evidence for the mechanism of action of MMV-08138 via targeting of IspD, an enzyme in the key isoprenoid precursor biosynthesis pathway in the apicoplast.

Materials and methods

Chemicals

Racemic MMV-08138 was purchased from Sigma. Diastereomers of MMV-08138 were purchased as custom syntheses from NuChem Therapeutics; enantiopurity was verified by HPLC-UV.

P. falciparum cultures

Plasmodium falciparum W2 (MRA-157), D10 (MRA-201), and D10 ACP_L-GFP (MRA-568) were obtained from MR4. Parasites were grown in human erythrocytes (2% hematocrit) in RPMI 1640 media supplemented with 0.25% Albumax II (GIBCO Life Technologies), 2 g/L

sodium bicarbonate, 0.1 mM hypoxanthine, 25 mM HEPES (pH 7.4), and 50 µg/L gentamicin, at 37 °C, 5% O_2, and 6% CO_2. For D10 ACP_L-GFP, the media was also supplemented with100 nM pyrimethamine (Sigma). For passage of drug-treated, IPP-rescued parasites, the media was supplemented with 5 µM drug and 200 µM IPP (Isoprenoids LC). For comparison of growth between different treatment conditions, cultures were carried simultaneously and handled identically with respect to media changes and addition of blood cells.

Growth inhibition assays

125 µL *P. falciparum* W2 cultures were grown in 96-well plates containing serial dilution of drugs in triplicate. Media was supplemented with 200 µM IPP as indicated. Growth was initiated with ring-stage parasites at 1% parasitemia and 0.5% hematocrit. Plates were incubated for 72 h. Growth was terminated by fixation with 1% formaldehyde and parasitized cells were stained with 50 nM YOYO-1 (Invitrogen). Parasitemia was determined by flow cytometry. Data were analyzed by BD C6 Accuri C-Sampler software, and EC_{50} curves plotted by GraphPad Prism. For reporting EC_{50} values, fresh drug stocks made from dry powder were used to minimize loss of efficacy of the compound during storage in solution.

Selection of drug-resistant mutants

Selection 1. P. falciparum W2 cultures were grown as described above in 6-well culture plates. Each well contained 10 mL of culture media at 2% hematocrit (Hct) and a starting parasitemia (% P) of 5%. On Day 0, cultures were treated with 9.3 µM MMV-08138 (Sigma; racemic mix), a concentration equal to 12x the EC_{50}. The parasites were maintained under drug pressure with daily media change and cultures were split 1:2 and supplemented with fresh

erythrocytes every 7 days. Parasite growth was monitored 2 times a week until ring-stage parasites were observed.

Selection 2. A two-step resistance selection was carried out as follows. A culture of W2 parasites (500 mL, 2% Hct, 15% P, ~1.5 $*10^{10}$ parasites) were treated with IC_{75} (600 nM) of the 1R,3S diastereomer of MMV-08138. After 7 days of daily media changes, no parasites were visible on a Giemsa-stained smear. The culture was maintained with media changes every 3 days and split 1:2 with fresh erythrocytes. Resistant parasites were observed emerging on day 43 of the treatment and on day 49 a split of the resistant line was seeded (50 mL, 2% Hct, 7.6% P, ~$8*10^8$ parasites) in a standard T-150 flask with treatment increased to 6 µM, or 30*EC_{50}, of 1R, 3S diastereomer of MMV-08138. After 7 days of daily media changes, no parasites were visible on a GIEMSA-stained smear and the culture was maintained henceforth with media changes every 3 days. On day 75, a resistant line emerged in the stepped-up split with visible growth defects that disappeared when the treatment was reduced to 2 µM of the 1R,3S diastereomer of MMV-08138. Concentrations were adjusted according to EC_{50} measurements on drug stocks used in the selection and may differ slightly from the reported EC_{50} on freshly-made drug stocks.

Genomic DNA (gDNA) isolation

In order to isolate gDNA from drug-resistant parasites, parasitized cultures underwent two consecutive cycles of synchronization (per 5% sorbitol treatment). Once highly synchronous (>90% ring-stage) and at 10% parasitemia, parasites were extracted by lysing RBCs with 0.1% saponin (Sigma) for 5 minutes. Intact parasites were washed twice with PBS and resuspended in 150 mM NaCl, 10 mM EDTA, 50 mM Tris pH 7.5 buffer. Subsequently, resuspended parasites were lysed by incubating overnight at 37 °C by addition of 0.1% L-loril sarkosil (Teknova) and

200 µg/mL Proteinase K (NEB). Following parasite lysis, nucleic acids were extracted with phenol/chloroform/isoamyl alcohol (25:24:1) pH 7.88 – 7.92 (Ambion) using phase-lock tubes (5 Prime). RNA was digested with 100 µg/mL RNAse A (Qiagen) treatment for 1 h at 37 °C. Subsequently, gDNA was extracted twice more as described above and once with 100% chloroform. Ethanol precipitation was carried out using conventional methods and purified gDNA was stored at -20 °C.

Whole-genome sequencing

Illumina-compatible 131nt paired-end libraries were made from 25 ng of purified gDNA using Nextera DNA Sample Prep Kit (Epicentre) per the supplier's instructions (however, the bPCR step was decreased to 6 cycles from 9 cycles with a modified extension step to 60 °C for 6 min). Additionally, Illumina-compatible adaptors were included at this PCR step in place of Nextera Adapter 2. Library fragments from 360 to 540 bp were size-selected on a 5 XT DNA 750 chip via the Lab Chip XT system (Caliper Life Sciences). Finally, a second PCR step using Klentaq LA DNA Polymerase (Sigma-Aldrich) and 80% A/T dNTPs was performed with the outer sequencing adaptors for 6 cycles (with an extension at 60 °C for 6 min) to enrich for library fragments that were primed for sequencing. Preceding cluster generation, library concentrations were confirmed by qPCR using Nextera adaptor sequences.

Pooled genomic DNA libraries at 2 nM each were sequenced on an Illumina HiSeq-2500. Cluster generation was performed via the cBot HiSeq Cluster Kit v2 from Illumina at a final concentration of 6-8 pM and density of >400 k/mm^2. Raw reads, consisting of 131nt paired-end sequences, were filtered for low quality reads, using the PriceSeqFilter module, available as a component of the PRICE metagenomic assembler software package and publicly available at

(derisilab.ucsf.edu/software/PRICE/) (21). Reads with an average per base quality score of <1% probability of an incorrect base were retained and then mapped to the 3D7 reference genome (PlasmoDB release 9.3) using the short read alignment software bowtie, keeping reads that were uniquely mapping with no more than a single mismatch, excluding five nucleotides trimmed from both ends of each read. Following mapping, alignments were evaluated for the presence of copy number variants (CNVs) and mutations. For CNVs and coverage calculations, the R-package "CNV-Seq" was used in conjunction with samtools to detect amplifications or deletions with a p-value of <0.001, using a 3 kb sliding window relative to the parental strain used to initiate each drug selection (22, 23). For mutation detection, a custom written python package (available upon request) was used to compare each bowtie alignment in the drug selected strain relative to the parental strain and the 3D7 reference genome. For each detected variant, the number of reads featuring that variant is reported, as well as the percentage of the total reads for that nucleotide position and variant. Only variants covered by a depth of 30 or more reads were considered reliable.

Sanger sequencing

The plasmodium IspD gene was PCR amplified from genomic DNA using the primer pair, 0.5F and 8R. PCRs contained 0.5 µM primers, 0.2 mM dNTPs (80% AT), 0.04 U/µL Phusion polymerase, and 1.5 ng/µL gDNA. Thermocycling conditions were 94 °C for 3 min; 30 cycles of 94 °C for 30 s, 55 °C for 30 s, and 60 °C for 5 min; final elongation of 60 °C for 20 min. The resulting IspD PCR product was Sanger sequenced. Primer sequences were as follows:

0.5F 5'-GGCATAAATATATGCACACAC-3'

1R 5'-TAC ACA TTT ATA CTG TGG AT-3'

2F 5'-GAG AGA AGT ATC AGA AAA TG-3'

3F 5'-TAT TAT GTG GAG GTA TAG GA-3'

3R 5'-TTC CAC TTT CTA CAA TTT TT-3'

4F 5'-ATT TTT CAT GTA TCA TCC AC-3'

4R 5'-ATT AAC ATC TTC AAA TTC GT-3'

5F 5'-AAT GTG ATC AAG ATG AAA AA-3'

6F 5'-ACG AAT TTG AAG ATG TTA AT-3'

6R 5'-TTT AAT AAA AGG GCT AGT TG-3'

7F 5'-TTC AAA AGC TAC AGA TAC TA-3'

8R 5'-CATATCGAATTTAAGAATGCG-3'

Cloning of a truncated *P. falciparum* IspD fusion protein for expression in *E. coli*

The plasmodium IspD gene was PCR amplified from wild type W2 genomic DNA as described above for Sanger sequencing using the following primer pair:

5'-CAAGCATATGCTCGAGGGGATGCATTTTGTTCATACG-3'

5'-TTAGCAGCCGGATCCTCATTTTGAAGAATAATAAAATTTGTG-3'

The resulting PCR product was purified using a Zymo DNA Clean & Concentrator-5 column (Zymo Research) and cloned using an In-Fusion PCR Cloning Kit (Clontech Laboratories, Inc.) into the XhoI site of a pET-19b T7 expression vector. The first 178 amino acids of IspD were then truncated using a QuikChange Lightning Site-Directed Mutagenesis Kit (Agilent Technologies) and the following primer pair:

5'-GACGACAAGCATATGCTCGAGGGGTTTAATAAATATAATACAAAACAAT-3'

5'-ATTGTTTTGTATTATATTTATTAAACCCCTCGAGCATATGCTTGTCGTC-3'

The truncated IspD was then PCR amplified from the pET-19b vector using the following primer pair:

5'-TACTTCCAATCCAATTTTAATAAATATAATACAAAACAATATG-3'

5'-TTATCCACTTCCAATTCATTTTGAAGAATAATAAAATTTGTG-3'

The purified PCR product was In-Fusion cloned into the SspI site of vector 1C from the QB3 Macrolab (http://qb3.berkeley.edu/qb3/macrolab/), encoding for an N-terminal His_6-Maltose Binding Protein-N_{10}-TEV protease site fusion tag (Pf-IspD-1C). This T7 expression system vector containing the IspD fusion was then transformed into BL21-CodonPlus (DE3)-RIL Competent Cells (Agilent Technologies, Inc.).

Expression of the PfIspD fusion protein in *E. coli*

Overnight cultures were used to inoculate a 1 L LB/KAN/CHL culture for protein expression at 37 °C. Induction was initiated with 1 mM Isopropyl β-D-1-thiogalactopyranoside (IPTG) at an OD_{600} of 0.5 and protein expression allowed to proceed for 3.5 h. Bacterial cells were harvested by centrifugation at 7000 g, and the cell pellet was suspended in 50 mM phosphate buffer, 300 mM NaCl, 20 mM imidazole, pH 8.0 containing lysozyme (1 mg/ml), and Complete EDTA-free protease inhibitor tablet (Roche) (one tablet per 25 mL buffer). Cells were incubated for 30 min at rt and then disrupted by sonication (20% amplitude, 6 bursts of 10 s with cooling in an ice bath for 10 s between each burst). After centrifugation at 20,000 g for 30 min at 4 °C, the supernatant was recovered and loaded onto a HisTrap HP 1 mL column (GE Healthcare Life Sciences) equilibrated in 50 mM phosphate buffer, 300 mM NaCl, and 20 mM imidazole using an AKTApure chromatography system. The column was washed

with the same buffer and eluted using an imidazole gradient (20–500 mM). Fractions were monitored for protein content by measuring absorbance at 280 nm and analyzed by SDS–polyacrylamide gel electrophoresis (SDS-PAGE) and silver staining. Fractions containing the crude desired IspD fusion were pooled and concentrated to 250 µL using an Amicon Ultra-4 centrifugal filter with a 30 kDa MWCO (EMD Millipore). The crude protein was loaded onto a HiLoad 16/60 Superdex 200 gel filtration column (GE Healthcare) pre-equilibrated with 100 mM Tris-HCl pH 8.0 buffer. The column was eluted at a flow rate of 1 mL/min and fractions monitored for protein content by measuring absorbance at 280 nm and analyzed by SDS–PAGE and silver staining. The fraction containing the desired IspD fusion was isolated, concentration determined using a BCA assay kit (Pierce Biotechnology, Inc.), and stored at 4 °C until further use. The recombinant Pf IspD protein sequence was confirmed by peptide sequencing with tandem liquid chromatography mass spectrometry (LC-MS/MS) of trypsin-digested gel bands from the preparation.

Activity measurements of *P. falciparum* IspD fusion protein

The enzymatic activity of IspD was measured using an EnzChek Pyrophosphate Assay Kit (Life Technologies) adapted for a 96-well plate microplate format, allowing for continuous monitoring of enzyme activity at pH 8.0 by measuring absorbance (360 nm) on a SpectraMax plate reader. Assay components were combined with enzyme (70.8 nM) and CTP (1 mM) in 200 µL reaction volume and allowed to pre-equilibrate to 37 °C for 10 min. The reaction was initiated by addition of 2C-methyl-D-erythritol-4-phosphate (MEP) (0-400 µM). Initial rates and kinetic parameters were calculated using GraphPad Prism (GraphPad Software). Enzyme activity at saturating MEP concentrations was also assayed in the presence of varying

concentrations of MMV-08138 stereoisomers which were added to the reaction before pre-equilibration.

Results

IPP rescue of MMV-08138 inhibition does not result in apicoplast loss

The Medicines for Malaria Venture (MMV) Open-Access Malaria Box is a diverse library of 200 drug-like anti-malarial compounds and 200 probe-like compounds compiled from 20,000 hits generated from previously reported large-scale screens (13–15). Previously, a screen for Malaria Box compounds showing IPP rescue phenotype identified MMV-08138, indicating that it specifically targets an apicoplast pathway (Figure 1A; (20, 24). We confirmed the IPP rescue phenotype of MMV-08138, which had an EC_{50}=772 nM (664-741 nM) against *P. falciparum* W2 strain in the absence of IPP but in the presence of IPP was at least 50-fold less potent with EC_{50} ≥50 μM (Figure 1B). The robust IPP rescue phenotype was also demonstrated by monitoring the growth of drug-treated parasites over several intra-erythrocytic cycles. During the first cycle of treatment, MMV-08138 blocked the maturation of trophozoite parasites to schizonts and then subsequent reinvasion at 24-48 h (Figure 1C). By contrast, in the presence of IPP, drug-treated parasites underwent continued growth and replication (Figure 1C). Of note, parasites treated with MMV-08138 and rescued with IPP do not become dependent on IPP for growth after removal of the drug (Figure 1C) or show a decrease in apicoplast:nuclear genome ratio (Figure S1). Localization of apicoplast-targeted GFP expressed in transgenic D10 ACP_L-GFP parasites was also unaffected (Figure S2) (25). Thus, unlike prokaryotic translation inhibitors such as doxycycline and chloramphenicol, neither organellar genome expression nor

organelle replication is affected by MMV-08138. The "immediate" death phenotype of MMV-08138 and maintenance of the apicoplast during drug treatment and IPP rescue is most consistent with an inhibition of apicoplast metabolic pathways, rather than housekeeping, protein import, or organelle replication functions (18, 26).

MMV-08138 inhibition is stereospecific

A set of 29 compounds, which were structurally related to MMV-08138 but with unknown stereochemistry, was also tested for antimalarial growth inhibition and IPP rescue (Figure S3; Table S1). These compounds were all less active than MMV-08138, either due to alterations in important functional groups or improper stereochemistry. Notably, MMV-08138 contains 2 stereocenters resulting in 4 possible diastereomers of this compound. Evaluation of its activity had thus far been carried out with an unspecified racemic mixture that could contain both active and inactive diastereomers (Figure 1). However, knowledge of the stereospecificity of the inhibitor will be important for further structure-activity optimization and *in vivo* studies. Therefore, we obtained all 4 chirally-pure diastereomers and evaluated each for its IPP-rescued growth inhibitory activity (Table 1; Figure S4). The most active compound was the 1R,3S conformer with an EC_{50} of 110 nM which showed IPP rescue up to 25 μM. The 1R,3R conformer was at least 30-fold less active but still showed IPP rescuable activity up to 25 μM. The 1S,3R conformer inhibited growth at EC_{50} 18.6 μM which was minimally rescued with IPP. Finally, the 1S,3S conformer was completely inactive. The stereospecificity of the growth inhibition indicated drug binding to a specific cellular target.

MMV-08138-resistant populations can be selected under drug pressure

In order to clarify the mechanism of action of MMV-08138, parasites resistant to MMV-08138 were generated in 2 independent selections (Figure 2A). In the first selection, susceptible blood-stage *P. falciparum* parasites were directly exposed to a lethal dose of a racemic mixture of MMV-08138. Resistant parasites emerged after 20 days of continuous drug exposure. The resistant population from this selection, designated 08138R1, was determined to have an EC_{50} that was 12.7-fold greater than the EC_{50} of the initial susceptible population against the 1R,3S diastereomer of MMV-08138 (Figure 2B). In the second selection, susceptible parasites were exposed to the 1R,3S diastereomer of MMV-08138 at a dose equal to IC_{75}. Resistant parasites, designated 08138R2, emerged after 43 days of continuous drug exposure and were found to have EC_{50} that was 3.5-fold greater than that of the initial susceptible population (Figure 2B). These 08138R2 parasites were then exposed to a lethal dose of MMV-08138 to generate a population, 08138R3, with EC_{50}=19.2-fold greater than that of the initial population after a total of 75 days of continuous drug exposure (Figure 2B).

Whole-genome sequencing of drug-resistant populations identifies mutations in IspD

Each of these 3 drug resistant populations, 08138R1, 08138R2, and 08138R3, and parent W2 strains used to begin each selection were subjected to whole genome sequencing. After quality filtering and alignment to the reference sequence, the average coverage ranged from 136-fold to 366-fold for the 14 chromosomes, >1000-fold for the mitochondria, and >300-fold for the plastid. Each dataset was evaluated for the presence of copy number variants (CNVs), such as amplified regions**.** Other than the variable sequences proximal to the telomeres, no CNVs of significance ($p<0.001$) were detected relative to the drug sensitive parental strain (Table S2). Unlike other examples of drug resistance in *P. falciparum* (27), this result suggests that a simple

amplification of a drug target or resistance determinant was not responsible for the observed resistance in these three selections.

Using the mapped reads for each resistant population, genomic mutations were detected by comparison to the reference sequence and the parental strain. Our criteria for mutations relevant to the selection consisted of non-synonymous mutations in which >90% of the reads at that position were "mutant" with respect to the parent and reference. Mutations relative to the reference strain, but which were identical in both the parental strain and the selected populations, were not considered relevant. Using these criteria, we detected 3 non-synonymous mutations in 08138R1, 3 in 08138R2, and 2 in 08138R3 (Table 2). In all three resistant populations, the only mutated gene shared in common was PF3D7_0106900, which is the putative 2-C methyl-D-erythritol 4-phosphate cytidylyltransferase (IspD) enzyme of the MEP isoprenoid precursor pathway (Figure 3). One mutation found in 08138R2 was a change from glutamate to glutamine at position 688 in IspD. Another mutation was found in both 08138R1 and 08138R3, a change from leucine to isoleucine at position 244 of IspD.

To confirm the presence of the identified mutations in IspD, the gene was PCR amplified from genomic DNA of the parent and resistant populations and the entire gene sequenced using the Sanger method (Figure S5). All the IspD mutations observed in the whole genome sequencing data were validated by Sanger sequencing (Figure 3A). In the case of population 08138R2, which was only selected to 91% mutant call purity, the PCR amplification product of IspD was cloned into a vector, transformed into *E. coli*, and 11 colonies selected for sequencing. Ten colonies showed the E688Q mutation while one colony did not show the mutation, in agreement with the whole genome sequencing data. Several mutations relative to the reference strand were also shared by both the parental and selected populations (Figure S6). This data

supports the notion that the anti-apicoplast action of MMV8138 is due to inhibition of this critical isoprenoid precursor biosynthesis enzyme, given that mutations in this gene suppress its activity. A block level amino acid alignment of *P. falciparum* IspD with those from *E. coli* and *A. thaliana* shows that PfIspD contains significant additional domains of unknown utility (Figure 3B). However, both of the reported mutations do occur proximal to conserved regions among the homologs of IspD.

MMV-08138 inhibits *P. falciparum* IspD activity *in vitro*

To determine if MMV-08138 directly inhibits PfIspD, we heterologously expressed and purified His and MBP-tagged PfIspD and measured its enzymatic activity using a pyrophosphate release assay. The purified enzyme was active with a K_m of 60.6 µM for MEP and a k_{cat} of 0.16 s^{-1} (Figure S7). In the presence of varying amounts of the 1R,3S-diastereomer of MMV-08138, enzyme activity measured at saturating substrate concentrations was inhibited with an IC_{50} of 7.0 nM (Figure 4; Table 1). Inhibition by MMV-08138 of PfIspD activity was stereospecific as the other diastereomers of MMV-08138 were all less potent (Figure 4; Table 1). The IC_{50} was similar when PfIspD activity was measured at substrate concentrations equal to K_m, when the enzyme is not saturated (Figure S7).

Interestingly, MMV-08138 inhibits PfIspD activity but did not inhibit *E. coli, A. thaliana,* or *P. vivax* IspD activity *in vitro.* We tested MMV-08138 in *in vitro* activity assays against MEP pathway enzyme homologs from various organisms. MMV-08138 showed no enzyme inhibition against *E. coli* DXS at up to 100 µM inhibitor, DXR/IspC at up 50 µM, or IspD, IspE, and IspF at 10 µM (Figure S8; (28–31)). MMV-08138 also did not affect the enzyme activity of purified *A. thaliana* or *P. vivax* IspD at up to 1 mM inhibitor (Figure S9; (32, 33).

Discussion

Both the genetic and biochemical evidence identify PfIspD, an enzyme in the key MEP isoprenoid precursor biosynthesis pathway in the apicoplast, as the molecular target of MMV-08138. The determinants of resistance against MMV-08138 were two mutations in IspD. The E688Q mutation was identified in 3.5-fold "low" resistant strain. Meanwhile, two independent selections carried out with different protocols converged on the same L244I mutation, which was identified in both higher (13-19 fold) resistant strains. In all three resistant populations, the only mutated gene shared in common was IspD. Interestingly, the L244I yielded the higher resistance phenotype, yet is a more subtle amino acid change compared to E688Q. Small amino acid changes can result in pronounced resistance phenotypes, as an isoleucine-to-leucine mutation in acetyl-CoA carboxylases has previously been demonstrated to confer herbicide resistance in plants (34, 35).

Based on the genetic results, further biochemical characterization demonstrated that MMV-08138 acts by directly binding and inhibiting IspD enzymatic activity. Consistent with this mechanism, the IC_{50} of the inhibitor against purified PfIspD was comparable to the EC_{50} against blood-stage *P. falciparum* parasites. The stereospecificity of the enzyme inhibition also paralleled that of cell growth inhibition. Surprisingly, MMV-08138 did not inhibit the enzyme activity of purified *E. coli*, *A. thaliana*, or *P. vivax* IspD (28, 32). This may be due to structural differences in IspD homologs in these species, as even the *P. vivax* and *P. falciparum* IspD share only 31% identity. Further studies using the same detection assay and kinetic conditions to compare IspD homologs will be required to confirm the selectivity of MMV-08138 for IspD homologs from different species.

Further kinetic and structural characterization will be required to identify the mechanism of inhibition of PfIspD by MMV-08138. MMV-08138 may compete with substrate binding sites for either MEP or CTP. Alternatively, MMV-08138 may bind at an allosteric site that affects enzyme activity. IspD may have important interactions with small molecules or proteins at allosteric sites to regulate its function. For example, interaction of IspD with other MEP enzymes may be important for the flux of intermediates through the pathway and final product formation. In addition, feedback regulation by MEP pathway intermediates and isoprenoid products has been shown for IspF, another pathway enzyme (36). How the L244I and E688Q mutations result in resistance to inhibition by MMV-08138 will also be revealing.

MMV-08138 has promise for drug development, with potent nM activity against infected red blood cells, drug-like properties, and synthetically-accessible structural analogs to optimize for *in vivo* activity (19). In particular, we showed that the 1R,3S diastereomer of MMV-08138 is most potent, which will be important for its structural optimization and minimizing off-target effects *in vivo*. The apicoplast MEP pathway is a validated anti-malarial target. While fosmidomycin has promise as a MEP pathway inhibitor against malaria, its development as a drug has been hampered by its short half-life and high recrudescence rates clinically (8). MMV-08138 has significant value as an alternative chemical scaffold to fosmidomycin for development as an anti-malarial MEP inhibitor. To date, few compounds targeting IspD in any organism have been developed though the MEP pathway is a validated antibacterial and antimalarial target (32, 37) Notably, although humans do not have a functional MEP pathway, there is a human IspD homolog that is associated with Walker-Warburg syndrome, a congenital muscular dystrophy, and likely acts as a nucleotide-dependent glycosyltransferase (38, 39). Thus, it may be important to screen against binding to human IspD, although PfIspD and the human *ISPD* gene share

minimal sequence similarity (at most 20% identical over 102 residues that could be aligned by the Smith-Waterman algorithm). The heterologous expression and purification of active PfIspD will facilitate both high-throughput screening and structural biology efforts which may further aid in the advancement of this target toward a preclinical lead compound.

An advantage of developing apicoplast-specific inhibitors is that the organelle is also essential in liver and mosquito stages of infection, increasing the likelihood that the drug candidates will have activities against multiple stages of parasite's complex life cycle (6, 40–42). Current MMV guidelines for compound development demand transmission blocking capability as part of Target Candidate Profile 3, requiring a target vulnerable in sexual stages and dormant liver stages (43). The efficacy of an IspD inhibitor against sexual and liver stages will need to be determined. Furthermore, drug synergy with known apicoplast inhibitors, such as antibiotics or fosmidomycin, can also be explored (44). Notably, fosmidomycin resistant parasites remained susceptible to MMV-08138 (20), and cross-resistance with fosmidomycin was not observed for the selected MMV-08138 resistant populations (Figure S10). Finally, as apicoplasts are found in other Apicomplexan parasites, developed drugs might also be used for treatment of diseases caused by *T. gondii* and Babesia *spp* parasites.

In this work, the IPP chemical rescue phenotype and target elucidation identified an inhibitor against a validated pathway with known essential role in apicoplast biology. However, the same strategy has potential to reveal new pathways and targets we had not previously anticipated. Mechanism of action elucidation is facilitated by the availability of assays to interrogate specific apicoplast functions, in addition to unbiased methods such as drug resistance selection. Our previous work demonstrating that MEP isoprenoid precursor biosynthesis is the only essential function of the apicoplast in blood-stage *P. falciparum* had important implications

for development of small molecule inhibitors against the apicoplast (18). Besides MEP isoprenoid precursor biosynthesis itself, there are few "classic" metabolic pathways to target. Instead, we need to pursue "non-traditional" pathways that are involved in maintaining organelle function or replicating the organelle during the *Plasmodium* life cycle. Unfortunately, our knowledge of these pathways from candidate proteins to mechanism is scarce. Due to the apicoplast's "exotic" evolution as a secondary plastid, there are few counterparts in other model organisms as starting points to tackle this unique but challenging biology. The forward chemical genetics approach described herein is an opportunity to discover essential functions in the apicoplast that can be targeted by small molecules. These compounds will serve as starting points to 1) identify drug candidate leads with specificity for an apicoplast target, 2) develop chemical tools to probe apicoplast pathways, and 3) discover new pathway/protein targets in the apicoplast and novel modes of action.

Acknowledgements

We are grateful to Medicines for Malaria Ventures (MMV) for providing the Malaria Box compounds and making this valuable library freely available, as well as Novartis for their screening efforts that first identified MMV-08138. We acknowledge Boris Illarionov and Markus Fischer (Universität Hamburg) for *in vitro A. thaliana* and *P. vivax* IspD assays, Katie Heflin and Caren Meyers (Johns Hopkins) for *in vitro E. coli* MEP enzyme assays, Giselle Knudsen and Michael Winter (UCSF Mass Spectrometry Facility) for mass spectrometry assistance, and Kip Guy (St. Jude Children's Hospital) for MMV-08138 structural analogs.

Financial Disclosure

Funding support for this project was provided by the Stanford Consortium for Innovation, Design, Evaluation and Action (C-IDEA; EY), NIH 1K08AI097239 (EY), NIH 1DP5OD012119 (EY), the Burroughs-Wellcome Fund (EY), the Howard Hughes Medical Institute (JLD), and a grant from the Grand Challenges Explorations, an initiative of the Bill & Melinda Gates Foundation (WW).

References

1. WHO | World Malaria Report 2013. WHO.
2. Dondorp AM, Nosten F, Yi P, Das D, Phyo AP, Tarning J, Lwin KM, Ariey F, Hanpithakpong W, Lee SJ, Ringwald P, Silamut K, Imwong M, Chotivanich K, Lim P, Herdman T, An SS, Yeung S, Singhasivanon P, Day NPJ, Lindegardh N, Socheat D, White NJ. 2009. Artemisinin Resistance in Plasmodium falciparum Malaria. N. Engl. J. Med. 361:455–467.
3. Köhler S, Delwiche CF, Denny PW, Tilney LG, Webster P, Wilson RJ, Palmer JD, Roos DS. 1997. A plastid of probable green algal origin in Apicomplexan parasites. Science 275:1485–1489.
4. Janouškovec J, Horák A, Oborník M, Lukeš J, Keeling PJ. 2010. A common red algal origin of the apicomplexan, dinoflagellate, and heterokont plastids. Proc. Natl. Acad. Sci. 107:10949 –10954.
5. Dahl EL, Shock JL, Shenai BR, Gut J, DeRisi JL, Rosenthal PJ. 2006. Tetracyclines specifically target the apicoplast of the malaria parasite Plasmodium falciparum. Antimicrob. Agents Chemother. 50:3124.
6. Stanway R, Witt T, Zobiak B, Aepfelbacher M, Heussler V. 2009. GFP-targeting allows visualization of the apicoplast throughout the life cycle of live malaria parasites. Biol. Cell 101:415–430.
7. Jomaa H, Wiesner J, Sanderbrand S, Altincicek B, Weidemeyer C, Hintz M, Türbachova I, Eberl M, Zeidler J, Lichtenthaler HK, Soldati D, Beck E. 1999. Inhibitors of the nonmevalonate pathway of isoprenoid biosynthesis as antimalarial drugs. Science 285:1573–1576.
8. Wiesner J, Borrmann S, Jomaa H. 2003. Fosmidomycin for the treatment of malaria. Parasitol. Res. 90:71–76.
9. Borrmann S, Issifou S, Esser G, Adegnika AA, Ramharter M, Matsiegui P-B, Oyakhirome S, Mawili-Mboumba DP, Missinou MA, Kun JFJ, Jomaa H, Kremsner PG. 2004. Fosmidomycin-clindamycin for the treatment of Plasmodium falciparum malaria. J. Infect. Dis. 190:1534–1540.
10. Borrmann S, Adegnika AA, Matsiegui P-B, Issifou S, Schindler A, Mawili-Mboumba DP, Baranek T, Wiesner J, Jomaa H, Kremsner PG. 2004. Fosmidomycin-clindamycin for Plasmodium falciparum Infections in African children. J. Infect. Dis. 189:901–908.

11. Oyakhirome S, Issifou S, Pongratz P, Barondi F, Ramharter M, Kun JF, Missinou MA, Lell B, Kremsner PG. 2007. Randomized controlled trial of fosmidomycin-clindamycin versus sulfadoxine-pyrimethamine in the treatment of Plasmodium falciparum malaria. Antimicrob. Agents Chemother. 51:1869–1871.
12. Lanaspa M, Moraleda C, Machevo S, Gonzalez R, Serrano B, Macete E, Cistero P, Mayor A, Hutchinson D, Kremsner PG, Alonso P, Menendez C, Bassat Q. 2012. Inadequate Efficacy of a New Formulation of Fosmidomycin-Clindamycin Combination in Mozambican Children Less than Three Years Old with Uncomplicated Plasmodium falciparum Malaria. Antimicrob. Agents Chemother. 56:2923–2928.
13. Guiguemde WA, Shelat AA, Bouck D, Duffy S, Crowther GJ, Davis PH, Smithson DC, Connelly M, Clark J, Zhu F, Jiménez-Díaz MB, Martinez MS, Wilson EB, Tripathi AK, Gut J, Sharlow ER, Bathurst I, Mazouni FE, Fowble JW, Forquer I, McGinley PL, Castro S, Angulo-Barturen I, Ferrer S, Rosenthal PJ, DeRisi JL, Sullivan DJ, Lazo JS, Roos DS, Riscoe MK, Phillips MA, Rathod PK, Van Voorhis WC, Avery VM, Guy RK. 2010. Chemical genetics of Plasmodium falciparum. Nature 465:311–315.
14. Gamo F-J, Sanz LM, Vidal J, de Cozar C, Alvarez E, Lavandera J-L, Vanderwall DE, Green DVS, Kumar V, Hasan S, Brown JR, Peishoff CE, Cardon LR, Garcia-Bustos JF. 2010. Thousands of chemical starting points for antimalarial lead identification. Nature 465:305–310.
15. Rottmann M, McNamara C, Yeung BKS, Lee MCS, Zou B, Russell B, Seitz P, Plouffe DM, Dharia NV, Tan J, Cohen SB, Spencer KR, González-Páez GE, Lakshminarayana SB, Goh A, Suwanarusk R, Jegla T, Schmitt EK, Beck H-P, Brun R, Nosten F, Renia L, Dartois V, Keller TH, Fidock DA, Winzeler EA, Diagana TT. 2010. Spiroindolones, a potent compound class for the treatment of malaria. Science 329:1175–1180.
16. O' Connor CJ, Laraia L, Spring DR. 2011. Chemical genetics. Chem. Soc. Rev. 40:4332.
17. Kirk K. 2001. Membrane transport in the malaria-infected erythrocyte. Physiol. Rev. 81:495–537.
18. Yeh E, DeRisi JL. 2011. Chemical Rescue of Malaria Parasites Lacking an Apicoplast Defines Organelle Function in Blood-Stage Plasmodium falciparum. PLoS Biol 9:e1001138.
19. Spangenberg T, Burrows JN, Kowalczyk P, McDonald S, Wells TNC, Willis P. 2013. The Open Access Malaria Box: A Drug Discovery Catalyst for Neglected Diseases. PLoS ONE 8:e62906.
20. Bowman JD, Merino EF, Brooks CF, Striepen B, Carlier PR, Cassera MB. 2013. Anti-apicoplast and gametocytocidal screening to identify the mechanisms of action of compounds within the Malaria Box. Antimicrob. Agents Chemother. AAC.01500–13.
21. Ruby JG, Bellare P, Derisi JL. 2013. PRICE: software for the targeted assembly of components of (Meta) genomic sequence data. G3 Bethesda Md 3:865–880.
22. Xie C, Tammi MT. 2009. CNV-seq, a new method to detect copy number variation using high-throughput sequencing. BMC Bioinformatics 10:80.
23. Li H, Handsaker B, Wysoker A, Fennell T, Ruan J, Homer N, Marth G, Abecasis G, Durbin R, 1000 Genome Project Data Processing Subgroup. 2009. The Sequence Alignment/Map format and SAMtools. Bioinforma. Oxf. Engl. 25:2078–2079.
24. ChEMBL-NTD | ChEMBL - Neglected Tropical Disease.
25. Waller RF, Reed MB, Cowman AF, McFadden GI. 2000. Protein trafficking to the plastid of Plasmodium falciparum is via the secretory pathway. EMBO J. 19:1794–1802.

554 26. Ramya TNC, Mishra S, Karmodiya K, Surolia N, Surolia A. 2007. Inhibitors of
555 nonhousekeeping functions of the apicoplast defy delayed death in Plasmodium
556 falciparum. Antimicrob. Agents Chemother. 51:307–316.
557 27. Guler JL, Freeman DL, Ahyong V, Patrapuvich R, White J, Gujjar R, Phillips MA, DeRisi J,
558 Rathod PK. 2013. Asexual Populations of the Human Malaria Parasite, Plasmodium
559 falciparum, Use a Two-Step Genomic Strategy to Acquire Accurate, Beneficial DNA
560 Amplifications. PLoS Pathog 9:e1003375.
561 28. Majumdar A, Shah MH, Bitok JK, Hassis-LeBeau ME, Freel Meyers CL. 2009. Probing
562 phosphorylation by non-mammalian isoprenoid biosynthetic enzymes using 1H–31P–
563 31P correlation NMR spectroscopy. Mol. Biosyst. 5:935.
564 29. Brammer LA, Smith JM, Wade H, Meyers CF. 2011. 1-Deoxy-D-xylulose 5-phosphate
565 synthase catalyzes a novel random sequential mechanism. J. Biol. Chem. 286:36522–
566 36531.
567 30. Brammer LA, Meyers CF. 2009. Revealing substrate promiscuity of 1-deoxy-D-xylulose
568 5-phosphate synthase. Org. Lett. 11:4748–4751.
569 31. Smith JM, Warrington NV, Vierling RJ, Kuhn ML, Anderson WF, Koppisch AT, Freel
570 Meyers CL. 2014. Targeting DXP synthase in human pathogens: enzyme inhibition and
571 antimicrobial activity of butylacetylphosphonate. J. Antibiot. (Tokyo) 67:77–83.
572 32. Kunfermann A, Witschel M, Illarionov B, Martin R, Rottmann M, Höffken HW, Seet M,
573 Eisenreich W, Knölker H-J, Fischer M, Bacher A, Groll M, Diederich F. 2014. Pseudilins:
574 Halogenated, Allosteric Inhibitors of the Non-Mevalonate Pathway Enzyme IspD.
575 Angew. Chem. Int. Ed Engl.
576 33. Witschel MC, Höffken HW, Seet M, Parra L, Mietzner T, Thater F, Niggeweg R, Röhl F,
577 Illarionov B, Rohdich F, Kaiser J, Fischer M, Bacher A, Diederich F. 2011. Inhibitors of
578 the Herbicidal Target IspD: Allosteric Site Binding. Angew. Chem. Int. Ed. 50:7931–
579 7935.
580 34. Christoffers MJ, Berg ML, Messersmith CG. 2002. An isoleucine to leucine mutation in
581 acetyl-CoA carboxylase confers herbicide resistance in wild oat. Genome Natl. Res.
582 Counc. Can. Génome Cons. Natl. Rech. Can. 45:1049–1056.
583 35. Délye C, Wang T, Darmency H. 2002. An isoleucine-leucine substitution in
584 chloroplastic acetyl-CoA carboxylase from green foxtail (Setaria viridis L. Beauv.) is
585 responsible for resistance to the cyclohexanedione herbicide sethoxydim. Planta
586 214:421–427.
587 36. Bitok JK, Meyers CF. 2012. 2C-Methyl-d-erythritol 4-phosphate enhances and sustains
588 cyclodiphosphate synthase IspF activity. ACS Chem. Biol. 7:1702–1710.
589 37. Gao P, Yang Y, Xiao C, Liu Y, Gan M, Guan Y, Hao X, Meng J, Zhou S, Chen X, Cui J. 2012.
590 Identification and validation of a novel lead compound targeting 4-diphosphocytidyl-
591 2-C-methylerythritol synthetase (IspD) of mycobacteria. Eur. J. Pharmacol. 694:45–52.
592 38. Roscioli T, Kamsteeg E-J, Buysse K, Maystadt I, van Reeuwijk J, van den Elzen C, van
593 Beusekom E, Riemersma M, Pfundt R, Vissers LELM, Schraders M, Altunoglu U,
594 Buckley MF, Brunner HG, Grisart B, Zhou H, Veltman JA, Gilissen C, Mancini GMS,
595 Delrée P, Willemsen MA, Ramadža DP, Chitayat D, Bennett C, Sheridan E, Peeters EAJ,
596 Tan-Sindhunata GMB, de Die-Smulders CE, Devriendt K, Kayserili H, El-Hashash OAE-
597 F, Stemple DL, Lefeber DJ, Lin Y-Y, van Bokhoven H. 2012. Mutations in ISPD cause
598 Walker-Warburg syndrome and defective glycosylation of α-dystroglycan. Nat. Genet.
599 44:581–585.

39. Willer T, Lee H, Lommel M, Yoshida-Moriguchi T, de Bernabe DBV, Venzke D, Cirak S, Schachter H, Vajsar J, Voit T, Muntoni F, Loder AS, Dobyns WB, Winder TL, Strahl S, Mathews KD, Nelson SF, Moore SA, Campbell KP. 2012. ISPD loss-of-function mutations disrupt dystroglycan O-mannosylation and cause Walker-Warburg syndrome. Nat. Genet. 44:575–580.
40. Nagaraj VA, Sundaram B, Varadarajan NM, Subramani PA, Kalappa DM, Ghosh SK, Padmanaban G. 2013. Malaria parasite-synthesized heme is essential in the mosquito and liver stages and complements host heme in the blood stages of infection. PLoS Pathog. 9:e1003522.
41. Vaughan AM, O'Neill MT, Tarun AS, Camargo N, Phuong TM, Aly AS., Cowman AF, Kappe SH.. 2009. Type II fatty acid synthesis is essential only for malaria parasite late liver stage development. Cell. Microbiol. 11:506–520.
42. Yu M, Santha Kumar TR, Nkrumah LJ, Coppi A, Retzlaff S, Li CD, Kelly BJ, Moura PA, Lakshmanan V, Freundlich JS, Valderramos J-C, Vilcheze C, Siedner M, Tsai JH-C, Falkard B, Sidhu A bir S, Purcell LA, Gratraud P, Kremer L, Waters AP, Schiehser G, Jacobus DP, Janse CJ, Ager A, Jacobs WR, Sacchettini JC, Heussler V, Sinnis P, Fidock DA. 2008. The Fatty Acid Biosynthesis Enzyme FabI Plays a Key Role In the Development of Liver Stage Malarial Parasites. Cell Host Microbe 4:567–578.
43. Burrows JN, Huijsduijnen RH van, Möhrle JJ, Oeuvray C, Wells TN. 2013. Designing the next generation of medicines for malaria control and eradication. Malar. J. 12:187.
44. Wiesner J, Henschker D, Hutchinson DB, Beck E, Jomaa H. 2002. In vitro and in vivo synergy of fosmidomycin, a novel antimalarial drug, with clindamycin. Antimicrob. Agents Chemother. 46:2889–2894.

Figure legends

Figure 1. IPP rescue of growth inhibition by MMV-08138. A. Chemical structure. B. EC_{50} curves in the absence and presence of IPP. C. Time course of growth through intraerythrocytic cycle. Parasites were treated with drug only, drug+IPP, or drug+IPP followed by removal of drug and IPP after the first reinvasion. Parasitemia is normalized to that of an untreated control.

Figure 2. Selection of MMV-08138 resistant parasite populations. A. Drug selection timeline. B. EC_{50} curves of resistant populations.

634 **Figure 3. Identification of IspD mutations in MMV-08138 resistant parasites.** A. Mutations
635 determined by whole genome and Sanger sequencing of resistant populations 08138R1, R2, and
636 R3. B. Block level alignment of *P. falciparum*, *A. thaliana*, and *E. coli* IspD with % homology
637 of each block. MMV-08138 resistant PfIspD mutation locations are denoted by arrows.
638
639 **Figure 4. Inhibition of PfIspD enzyme activity by diastereomers of MMV-08138**
640

641 **Tables**

642

643 **Table 1. Inhibition by diastereomers of MMV-08138 of parasite growth and PfIspD**
644 **enzyme activity**

	Parasite growth EC_{50} μM[a]		PfIspD activity IC_{50} μM[a]
Stereoisomer	**No rescue**	**+IPP**	
1S,3S	>50[b]	>50[b]	>25[c]
1R,3S	0.11 (0.10-0.12)	>25[c]	0.0071 (0.0061-0.0083)
1R,3R	3.8 (2.7-5.3)	>25[c]	0.17 (0.14-0.20)
1S,3R	18.6 (12.4-28.0)	>25[c]	2.5 (1.9-3.1)

646 [a] Mean (95% confidence interval)

647 [b] No inhibition observed at 50 μM, the highest concentration tested.

648 [c] Estimated based on partial inhibition observed.

649

650 **Table 2. Summary of whole genome sequencing results**

Resistant Population	Gene ID[a]	Description[b]	nt position	Base Call		Read Numbers		% Reads[d]		AA change
				WT[c]	Mut	WT	Mut	WT	Mut	
08138R1	**PF3D7_0106900**	**2-C-methyl-D-erythritol 4-phosphate cytidylyltransferase**	**730**	**T**	**A**	**227**	**320**	**99.6**	**99.4**	**L244I**
	PF3D7_1247500	putative protein kinase	2632	G	T	110	73	97.3	100	D878Y
	PF3D7_1456700	conserved Plasmodium protein	1384	G	A	280	413	93.9	96.4	E462K
08138R2	**PF3D7_0106900**	**2-C-methyl-D-erythritol 4-phosphate cytidylyltransferase**	**2062**	**G**	**C**	**85**	**69**	**100**	**91.3**	**E688Q**
	PF3D7_0302900	putative exportin	1620	A	T	154	91	61.7	97.8	E540D
	PF3D7_1478600	Plasmodium exported protein	1241	C	T	66	59	100	96.6	T414I
08138R3	**PF3D7_0106900**	**2-C-methyl-D-erythritol 4-phosphate cytidylyltransferase**	**730**	**T**	**A**	**151**	**188**	**100**	**100**	**L244I**
	PF3D7_1417400	cyclic nucleotide binding protein pseudogene	10270	G	T	112	94	55.3	100	E3424*

651 [a] PlasmoDB gene Identification number

652 [b] Basic gene description based on PlasmoDB functional assignments

653 [c] WT calls match 3D7 reference genome

654 [d] % Reads - Percent of reads corresponding to WT call and Mut call respectively

655

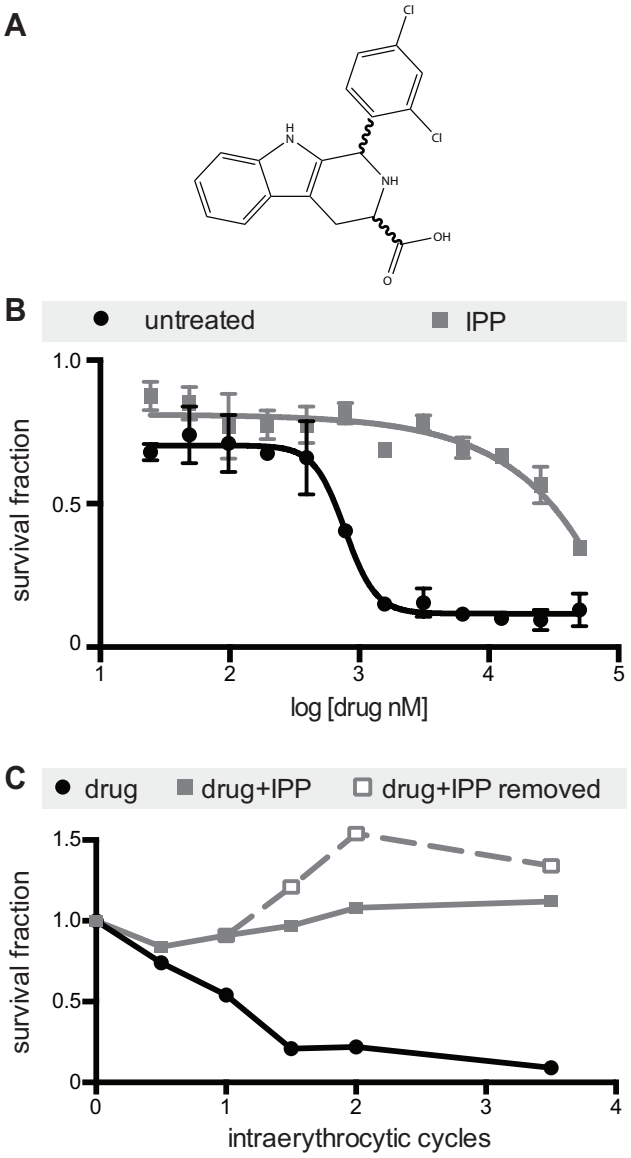

Figure 1. IPP rescue of growth inhibition by MMV-08138. A. Chemical structure. B. IC_{50} curves in the absence and presence of IPP. C. Time course of growth through intraerythrocytic cycle. Parasites were treated with drug only, drug+IPP, or drug+IPP followed by removal of drug and IPP after the first reinvasion. Parasitemia is normalized to that of an untreated control.

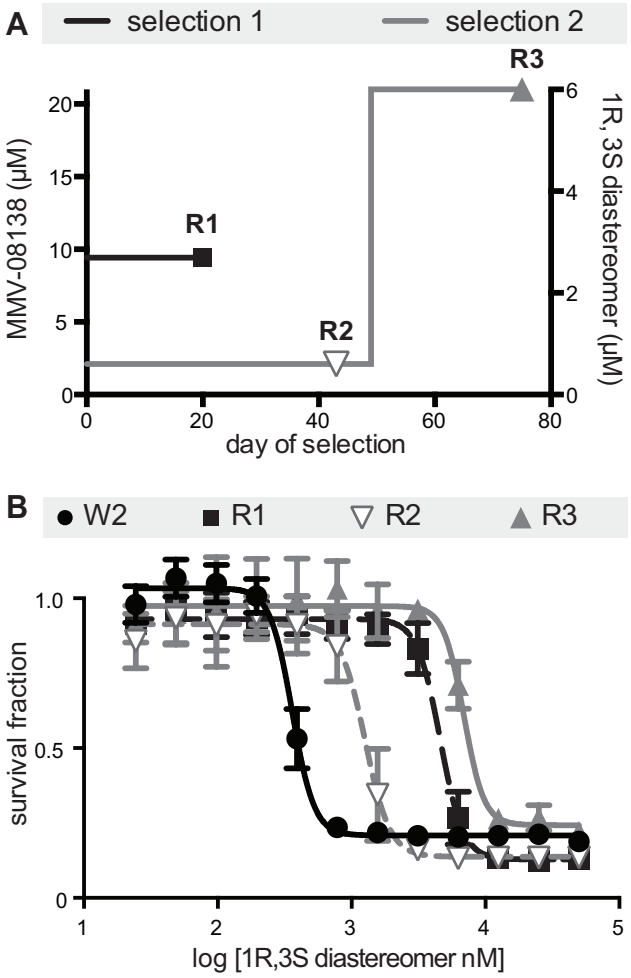

Figure 2. Selection of MMV-08138 resistant parasite populations. A. Drug selection timeline. B. EC_{50} curves of resistant populations.

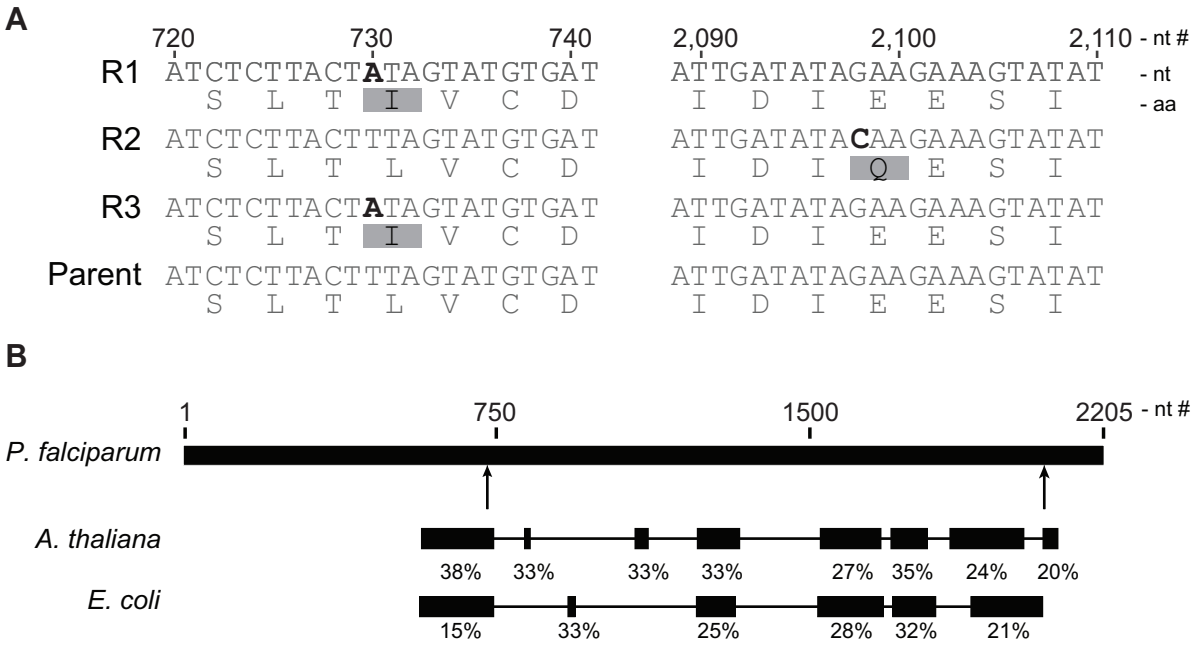

Figure 3. Identification of IspD mutations in MMV-08138 resistant parasites. A. Mutations determined by whole genome and Sanger sequencing of resistant populations 08138R1, R2, and R3. B. Block level alignment of *P. falciparum*, *A. thaliana*, and *E. coli* IspD with % homology of each block. MMV-08138 resistant PfIspD mutation locations are denoted by arrows.

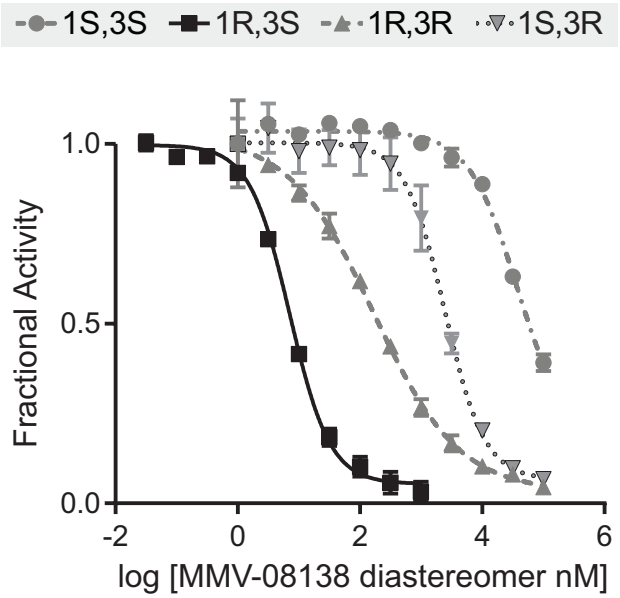

Figure 4. Inhibition of PfIspD enzyme activity by diastereomers of MMV-08138